The effect of nuclear spin waves on the magnetization of $MnCO_3$

1993 J. Phys.: Condens. Matter 5 4215

(http://iopscience.iop.org/0953-8984/5/25/011)

J. Phys.: Condens. Matter 5 (1993) 4215–4224. Printed in the UK

The effect of nuclear spin waves on the magnetization of $MnCO_3$

L E Svistov†‡, J Löw† and H Benner†

† Institut für Festkörperphysik, TH Darmstadt and SFB 185, D-6100 Darmstadt, Federal Republic of Germany

‡ Institute of Crystallography, Academy of Sciences, Moscow 117333, Russia

Received 1 September 1992, in final form 18 January 1993

Abstract. By means of a SQUID magnetometer we have investigated the change of magnetic moment ΔM caused by RF pumping at NMR frequency in the easy-plane antiferromagnet $MnCO_3$. It is shown that ΔM arises mainly from a non-thermal packet of nuclear k=0 magnons. A characteristic time T_3 describing the relaxation of these magnons into the whole nuclear dispersion branch was evaluated from the experimental data. We found that T_3 is much smaller than the spin–lattice relaxation time T_1, which means that the strongly excited nuclear system can be described by a separate spin temperature T_n. A relaxation mechanism for T_3 is discussed which could explain the observed field and temperature dependences of ΔM.

1. Introduction

Hyperfine interactions between electron and nuclear spins in magnetically ordered dielectrics give rise to two fundamental effects: first, the magnetic moment of the electron shell leads to a strong local field H_{loc} at the sites of the nuclei determining their frequency of free spin precession ω_{n0}. Second, there occurs a coupling between electron and nuclear spin oscillations. The corresponding collective oscillations of both subsystems can be considered as a new type of quasi-particles: *electron magnons*, the energy of which is renormalized due to the interaction with the nuclear subsystem, and *nuclear magnons* representing low-energy excitations which are mainly determined by the oscillation of nuclear spins acting as a perturbation on the low-frequency wing of the electron subsystem resonance [1]. The most remarkable feature of nuclear magnons distinguishing them from electron magnons is their existence in a paramagnetic system of nuclear spins in the presence of strong thermal fluctuations and weak polarization ($\simeq 1\%$). The interactions between the nuclear and electron subsystems can be discussed in terms of an indirect coupling between nuclear spins (Suhl–Nakamura coupling) [2] resulting in a correlation of their motion over considerable distances.

The concept of nuclear magnons proposed by de Gennes *et al* [1] has been applied to both ferro- and antiferromagnets. It was shown [3–5] that the most convenient objects for studying nuclear magnons are antiferromagnets with cubic symmetry or with easy-plane anisotropy such as $MnCO_3$. In $MnCO_3$ the spectra of the (low-energy) electron magnons and nuclear magnons have the form [3, 4, 6]

$$\omega_{e,k}^2 = \gamma_e^2[H(H + H_D) + H_\Delta^2(T) + \alpha^2 k^2] \tag{1a}$$

$$\omega_{n,k}^2 = \omega_{n0}^2[1 - \gamma_e^2 H_\Delta^2(T)/\omega_{e,k}^2] \tag{1b}$$

0953-8984/93/254215+10$07.50

where $\gamma_e = g\mu_B/\hbar = 17.8 \times 10^9$ s^{-1} kOe^{-1} denotes the electron gyromagnetic ratio, H the external magnetic field, $H_D = 4.4$ kOe a Dzyaloshinskiĭ field, and α the stiffness constant which is proportional to the exchange field $H_E = 320$ kOe (the stiffness constant in c_3-direction amounts to $\alpha_\parallel = 0.84 \times 10^{-5}$ kOe cm). $\omega_{n0} \equiv \gamma_n H_{loc} = 2\pi \times 640$ MHz is the NMR frequency of ^{55}Mn in the absence of dynamic hyperfine coupling. Here, the local field is essentially given by the hyperfine field $H_{loc} = AM_{sl}(T)$ which is proportional to the electron sublattice magnetization $M_{sl}(T)$. In the limit of small external fields $H \ll H_{loc}$ ($\simeq 600$ kOe) and low temperature $T \ll T_N$ ($= 32$ K) ω_{n0} remains temperature independent. $H_\Delta \simeq \sqrt{5.8\text{K}/T}$ kOe is the gap in the electron spectrum (see figure 1) resulting mainly from hyperfine interactions. Its temperature dependence follows from a Curie behaviour of the nuclear sublattice polarization: $H_\Delta^2 \sim m_{sl}(T) \sim 1/T$. The influence of high-frequency electron modes on the spectral and relaxation properties of the nuclear system will be neglected here. For small values of k the spectra of (1) sensitively depend on electron and nuclear spin polarizations. Applying a strong radio-frequency (RF) field h the nuclear spin system can substantially be overheated [1, 7] with respect to the lattice temperature T, according to the NMR saturation phenomenon. The corresponding shift of electron and nuclear dispersion branches is illustrated in figure 1.

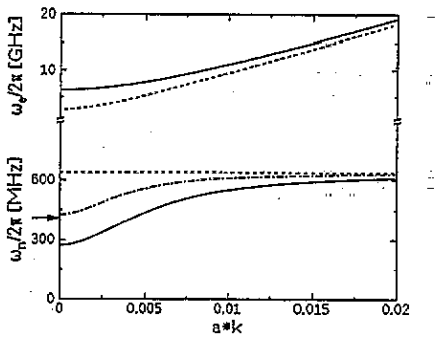

Figure 1. Electronic and nuclear branches of low-energy excitations in $MnCO_3$ in the absence (ω_{e0}, ω_{n0}; dashed line) and in the presence ($\omega_{e,k}, \omega_{n,k}$; full line) of dynamic hyperfine coupling ($H = 200$ Oe). The corresponding shift of the nuclear branch, the *frequency pulling*, depends sensitively on nuclear polarization. The frequency ω_p of the pumping field necessary to overheat the nuclear spin system from e.g. $T_n = 1.4$ K (full) to 5 K (dash-dotted) is marked with an arrow. The detuning between ω_p and $\omega_{n,k=0}(T_n)$ is in the order of the NMR linewidth.

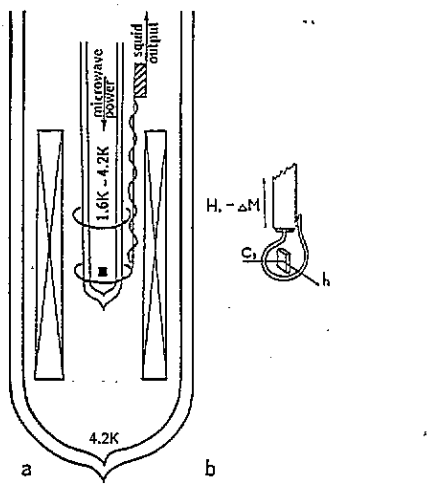

Figure 2. (a) Scheme of the low temperature part of the measuring device (see text). (b) Orientation of the RF field h, the static field H, the c_3-axis of the $MnCO_3$ crystal and the measured change of magnetic moment ΔM.

Strong RF pumping results in a non-thermal packet of nuclear magnons with $\omega_{n,k=0}(T_n) \simeq \omega_p$. The evolution of this packet is not yet known in detail. If relaxation processes inside the nuclear system are dominating the spin–lattice relaxation we expect a thermodynamic equilibrium defining a nuclear temperature $T_n > T$. In the opposite limit

this non-equilibrium packet will directly dissipate into the electron and phonon systems. Which of these two possible ways will be realized depends on the ratio between the spin–lattice relaxation time T_1 and a characteristic time necessary to reach the thermal equilibrium state in the nuclear spin subsystem, which we will call T_3.

The thermalization process (T_3 process) is a special one among several processes accounting for the relaxation of a nuclear magnon packet into all other degrees of freedom of the system. (The characteristic lifetime of the packet is normally denoted by T_2 and describes e.g. the linewidth in spectroscopic investigations.) The most probable nuclear magnon relaxation process [8–10] is based on their elastic scattering by fluctuations of the nuclear magnetic moments—sometimes referred to as $T_2(k)$ process—which, however, cannot thermalize the nuclear system. Theoretical analyses of other possible relaxation processes [10] which, in principle, could contribute to thermalization within the nuclear branch, however, are of no practical use to determine the values of T_1 and T_3.

Since the excitation of a single quasi-particle of energy $\epsilon_{i,k} = \hbar\omega_{i,k}$ gives rise to a well-defined change of magnetic moment according to $\mu_{i,k} = -\partial\epsilon_{i,k}/\partial H$ [5], it appeared promising to probe the evolution of non-thermal magnons by measuring the total change of magnetization induced by an external pumping field. In the present work we have experimentally studied the change of magnetic moment ΔM due to the excitation of non-thermal nuclear magnons. Their relatively low frequency allows one to probe the full frequency range of the nuclear magnon dispersion branch. Due to the weak coupling between the nuclear spins and the electron spins and phonons, an overheating of the nuclear system can already be obtained with rather low RF power, thus allowing measurements within a wide range of the nuclear temperature T_n.

2. Experimental details

For measuring the change of magnetic moment induced by the microwave field, we built a wide-band microwave spectrometer combined with a standard SQUID magnetometer. The device was designed to work in a frequency range from 100 kHz to 6 GHz, in a temperature range from 1.4 to 4.2 K and in magnetic fields up to 400 Oe.

We used a SQUID measuring cell of Zimmerman type [11] (constructed in the Institute of Geophysics of the Academy of Sciences of Russia, Novosibirsk) which shows a very good long-time stability. The flux transformer is of the gradiometer type to reduce external noise. The flux transformer and the SQUID cell are placed inside a liquid helium bath at 4.2 K. The static magnetic field H is applied by a superconducting solenoid which operates in the persistent mode. For thermal isolation of the sample a metal dewar was placed inside the flux transformer. Serving as a screen for microwave fields, the dewar allows the application of large RF or microwave powers to the sample without affecting the operating point of the SQUID. For external noise reduction we used additional superconducting screens. The RF field for exciting the nuclear spin system was applied thorugh a coaxial line matched by a coil with several turns. The orientation of the static field and of the RF field with respect to the c_3-axis of the crystal are shown in figure 2. The change of total magnetic moment ΔM was measured with a precision of 5×10^{-7} G cm^3. The absolute value of total magnetic moment M could be measured with a precision of 10% by moving the sample out of the measuring cell. In order to dispense with poorly defined scaling factors resulting from device and samples, we shall only discuss the relative change of magnetic moment $\Delta M/M$.

The $MnCO_3$ samples were small plates of $0.5 \times 1 \times 2$ mm^3 size with the largest natural faces corresponding to the magnetic easy plane. Our measurements were performed on two

crystals with different concentrations of magnetic Co^{2+} impurities (0.17 and 0.29 at.%). The impurity concentration was determined by means of an energy-dispersive analysis with x-rays (EDAX). From the magnetization curve $M(H)$ we checked that for $H > 60$ Oe both crystals were in the monodomain regime.

3. Results

The change of magnetic moment ΔM induced by the RF pumping field was measured as a function of both RF pumping frequency ω_p and amplitude h. The following data were obtained from the first crystal. In figure 3 we present the frequency dependence of $\Delta M/M$ for different values of output power at the RF generator. Since our data have not been corrected for the frequency dependence of transmission losses, periodic peaks occur at lower powers indicating the effect of cable resonances and, thus, a periodic variation of h within the exciting coil despite a constant RF power level fed into the device. While this effect is rather tedious and disturbing at low RF power, it can be utilized to probe saturation effects of ΔM occurring at higher power. If ΔM becomes saturated—the mechanism will be discussed below—it becomes insensitive to a variation of h, and the periodic peaks will disappear (see 0 dB curve below 640 MHz in figure 3).

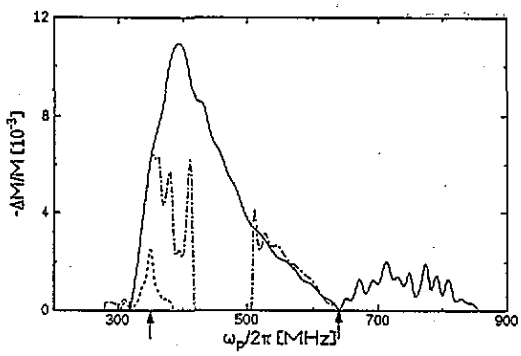

Figure 3. Relative change of magnetic moment as a function of pumping frequency ω_p for different output power of RF generator (——, 0 dB; — · —, −3 dB; – – –, −10 dB) and increasing frequency. The range of frequency pulling limited by $\omega_{n,k=0}(T)$ and ω_{n0} is marked with arrows. Peak structures at −3 dB and above 640 MHz result from cable resonances.

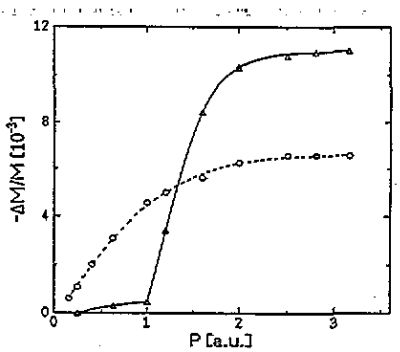

Figure 4. Dependence of $\Delta M/M$ on irradiated RF power P for different pumping frequencies: ○, resonant pumping, $\omega_p = \omega_n$; △, non-resonant pumping, $\omega_n < \omega_p < \omega_{n0}$ ($H = 400$ Oe and $T = 1.4$ K).

As a first and general result the curves can be divided into two parts. The first regime, ranging from roughly the low-power resonance position $\omega_{n,k=0}(T)$ at 350 MHz to the free precession limit ω_{n0} at 640 MHz, is related to an overheating of the nuclear spin system. The second regime occurring above 640 MHz is obviously connected with the process of parametric excitation of nuclear magnons by RF field components parallel to H (resulting e.g. from the inhomogeneity of h). This parallel pumping effect will be the subject of a subsequent paper and is not discussed in detail here. (In the following we replace $\omega_{n,k=0}(T_n = T)$ simply by ω_n.)

Figure 4 shows the dependence of $\Delta M/M$ on the irradiated RF power for resonant ($\omega_p = \omega_n$) and non-resonant ($\omega_n < \omega_p < \omega_{n0}$) pumping. For resonant pumping ΔM

shows a monotonic increase, whereas for non-resonant pumping at higher frequency a pronounced threshold behaviour is observed indicating that the non-linear overheating mechanism becomes efficient only above a certain RF amplitude.

The mechanism of saturation has been attributed [1,7] to an overheating process of the nuclear spin system shifting the nuclear frequency to an equilibrium position $\omega_n(T_n > T) \simeq \omega_p$. If ω_p is sufficiently close to ω_n, the nuclear spins of the whole sample are excited and the overheating process results in a uniform decrease of nuclear polarization which depends on the RF pumping power. Away from resonance ($\omega_n < \omega_p < \omega_{n0}$), where the uniform excitation would require an extremely high pumping level, a local overheating—in the neighbourhood of crystal imperfections or close to the surface—becomes more efficient, and we have two different contributions: an overheated one from these areas and a non-overheated one from the rest of the sample, which have both been probed e.g. by AFMR on the electron branch [1,7]. With increasing RF power a self-amplifying overheating takes place giving rise to the abrupt increase of ΔM described above. Saturation in this context means that the locally overheated areas cover the whole sample which again leads to the same uniform frequency ω_n coinciding with the pumping frequency ω_p. The crossover regime from 'almost resonant' to 'off-resonant' excitation depends on the width of the nuclear magnons and on sample quality and will complicate quantitative analyses.

Therefore, the following measurements and analyses were restricted to the limit of saturation. We checked this condition by double resonance experiments as reported in the literature [1,7]. In addition to the RF field pumping on the nuclear branch, a microwave field ranging in frequency from 3 to 8 GHz was fed into the same coil to probe the corresponding change in the electronic branch by AFMR. Again the AFMR signal was detected by measuring ΔM. Though the contribution to ΔM resulting from the electronic branch is much smaller ($\leqslant 5\%$) than the contribution from the nuclear branch the former could be singled out (at fixed ω_p) by sweeping the AFMR frequency. Applying sufficiently high RF power for exciting the nuclear mode (i) we observed a single AFMR line confirming uniform overheating and (ii) the observed *frequency pulling* of the AFMR line with respect to ω_p was found to be in qualitative agreement with the theoretical prediction of (1*a*). It is interesting to note that the detected change of magnetic moment ΔM due to AFMR strongly depends on ω_p and even changes its sign within a certain range of ω_p.

The relative change of magnetic moment observed at different temperatures (1.4 and 4.2 K) and constant RF generator output (0 dB) is shown in figure 5 with respect to the pumping frequency ω_p. In addition to the double resonance experiments the occurrence of saturation could be checked from the flattening of the periodic peak structures resulting from cable resonances. At higher magnetic field ($H = 400$ Oe, figure 5(b)) saturation was obtained within the whole frequency range of ω_p.

Analogous measurements were performed in the second crystal containing a larger amount of Co^{2+} impurities. We found that the RF threshold fields for overheating depend on sample quality, but the saturated curves $\Delta M(\omega_p)/M$ coincide within an accuracy of $\leqslant 10\%$. This fact indicates that the observed saturated values of ΔM are only connected with intrinsic properties of $MnCO_3$ and not with crystal imperfections.

4. Discussion

In the present limit of low fields and temperatures $T \ll T_N$ and $H \ll H_D$, H_{loc} the total magnetic moment of the sample mainly results from the canting of the two antiferromagnetic

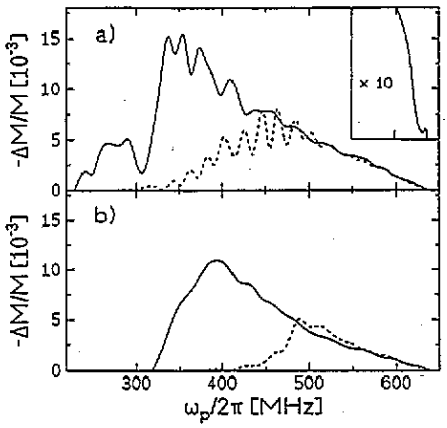

Figure 5. Relative change of magnetic moment $\Delta M/M$ with respect to pumping frequency ω_p for different temperatures (full line: 1.4 K, dashed: 4.2 K) and constant RF generator output (0 dB). (a) $H = 200$ Oe; saturation is obtained for $\omega_p/2\pi \geqslant 500$ MHz, as indicated by the flattening of cable resonances. (b) $H = 400$ Oe; saturation is obtained within the whole frequency range. Inset shows the small step at 640 MHz enlarged in scale.

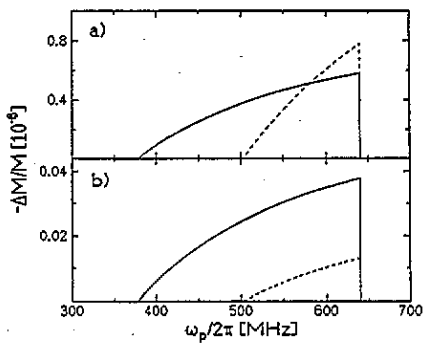

Figure 6. Change of magnetic moment ΔM with respect to ω_p for two different temperatures (full line: $T = 1.4$ K, dashed: 4.2 K) resulting from the change of thermal occupation. (a) Contribution of electron magnons according to (4) and (5). (b) Contribution of nuclear magnons according to (4) and (6).

sublattices (canting angle $\varphi \simeq H_D/H_E \simeq 0.8°$) and is given by

$$M = N_0 g \mu_B S H_D / H_E \tag{2}$$

where N_0 the total number of magnetic Mn^{2+} ions in the sample and $S = 5/2$. We now consider possible explanations of the observed change of magnetic moment ΔM induced by RF excitation of the nuclear mode.

As a first approach it is tempting to attribute the observed effect to a change Δm of total *nuclear* magnetic moment. Assuming a paramagnetic nuclear spin system in a local field H_{loc} we obtain

$$\Delta m \equiv 2[m_{sl}(T) - m_{sl}(T_n)]\frac{H_D}{H_E} = N_0 \frac{I(I+1)(\gamma_n \hbar)^2 H_{loc}}{3k_B}\frac{H_D}{H_E}\left(\frac{1}{T} - \frac{1}{T_n}\right) \tag{3}$$

where $I = 5/2$ is the nuclear spin of ^{55}Mn and $\gamma_n = 6.635 \times 10^7$ s^{-1} kOe^{-1} its gyromagnetic ratio. m_{sl} denotes the nuclear magnetic moment arising from either sublattice, and the factor H_D/H_E again results from the canting of the respective local fields. This contribution, however, remains far too small to be of importance.

Contributions from electron and nuclear magnons are considered in a rather general way by assuming that RF pumping results in a non-thermal packet of nuclear spin waves at $k = 0$, but all other excitations within either subsystem are in thermal equilibria. The overheating of the nuclear spin system gives rise to a shift of the electron and nuclear dispersion curves and, therefore, to a change of the occupation numbers of all corresponding magnons. The excitation of a quasi-particle with energy $\epsilon_{i,k} = \hbar\omega_{i,k}$ results in a magnetic moment $\mu_{i,k} = -\partial\epsilon_{i,k}/\partial H$ [5], where index i = e, n refers to the electron or nuclear magnon branches. Weighting the contribution of a single particle with the respective Bose factors

$n(T_i, \omega_{i,k})$ and assuming that the temperature of the electron spin system T_e is equal to the lattice temperature T the change of magnetic moment due to overheating the nuclear system can be written as

$$\Delta M = \sum_k \left\{\mu_{e,k}(T_n)n(T, \omega_{e,k}(T_n)) - \mu_{e,k}(T)n(T, \omega_{e,k}(T))\right\} + \sum_k \left\{\mu_{n,k}(T_n)n(T_n, \omega_{n,k}(T_n)) - \mu_{n,k}(T)n(T, \omega_{n,k}(T))\right\} + N\mu_{n,k\simeq 0}(\omega_p). \tag{4}$$

N denotes the number of non-thermal magnons of frequency ω_p excited by the RF field and by elastic scattering. Following (1) the change of magnetic moment due to the excitation of an electron magnon is given by

$$\mu_{e,k}(T_n) = -\tfrac{1}{2}\hbar\gamma H_D[H(H + H_D) + H_\Delta^2(T_n) + \alpha^2 k^2]^{-1/2} \tag{5}$$

while the excitation of a nuclear magnon yields a change of

$$\mu_{n,k}(T_n) = -\frac{\hbar\omega_{n0}H_D H_\Delta^2(T_n)}{2[H(H + H_D) + H_\Delta^2(T_n) + \alpha^2 k^2]^{3/2}[H(H + H_D) + \alpha^2 k^2]^{1/2}}. \tag{6}$$

The corresponding contributions to ΔM resulting from the change of thermal occupation are shown in figures 6(a) and (b) for two different temperatures.

Both contributions show a monotonic increase with temperature in contrast to our experimental data. Moreover, the absolute value of this effect is again too small to account for the observed results. Note, however, that both theoretical contributions show drastic jumps of ΔM at $\omega_p = \omega_{n0}$ the stronger one arising from the electron branch, which also seem to show up in our experimental data at $T = 4.2$ K (see inset in figure 5). The small step observed at 640 MHz is of the same order of magnitude as expected from figure 6(a).

The preceding analyses imply that the observed change of magnetic moment obviously cannot result from excitations which are in thermal equilibrium, but must be related to the non-thermal nuclear magnons which are directly excited by the RF pumping field, as described by the last RHS term of (4). In the stationary state the power absorbed by the nuclear spin system is balanced by the power dissipated from the nuclear spin system to the lattice. The dissipated power is determined by the spin–lattice relaxation time T_1 resulting in [1, 5]

$$P = 2[m_{sl}(T) - m_{sl}(T_n)]H_{loc}/T_1. \tag{7}$$

Here, $2m_{sl}(T_n)H_{loc}$ is the energy of the nuclear spin system. The term in brackets is the same as given in (3) but without the canting factor H_D/H_E accounting for the total moment. In order to evaluate the number of non-thermal nuclear magnons it is necessary to introduce a characteristic time T_3 describing the relaxation of the non-thermal wave packet to thermal equilibrium *inside* the nuclear spin system. Note that this assumption holds only for $T_3 \ll T_1$. The condition of balance of the energy flux leads to the following number of excited nuclear magnons:

$$N = (T_3/T_1)2[m_{sl}(T) - m_{sl}(T_n)]H_{loc}/(\hbar\omega_{n,k=0}). \tag{8}$$

Detailed evaluation of (4) results in the following expression

$$\Delta M = N\mu_{n,k=0}(T_n) = -\frac{T_3}{T_1}\frac{[m_{sl}(T) - m_{sl}(T_n)]H_{loc}H_\Delta^2(T_n)H_D}{H(H+H_D)[H(H+H_D)+H_\Delta^2(T_n)]}. \tag{9}$$

Combining (1*b*), (2) and (9) and taking into account the saturation condition $\omega_p \simeq \omega_n(T_n)$ we finally obtain

$$T_3/T_1 = -(\Delta M/M)A\omega_n^2(T)\omega_p^2/\{[\omega_p^2 - \omega_n^2(T)][\omega_{n0}^2 - \omega_p^2]\} \tag{10}$$

where factor A summarizing the remaining parameters of $MnCO_3$ amounts to a value of 5.1. Equation (10) allows the evaluation of T_3/T_1 with respect to T, H and ω_p directly from the experimental data.

The result of this evaluation is shown in figure 7. The analyses of field, temperature and frequency dependences can be summarized as follows.

(i) Within the whole parameter range investigated T_3, in fact, is much smaller than T_1, which is consistent with the assumption of a separate spin temperature T_n of the nuclear magnon system.

(ii) Within the temperature ranges 1.4 K $\leqslant T \leqslant$ 4.2 K and $T_n >$ 10 K the ratio T_3/T_1 is proportional to T.

(iii) By means of T_1 data on $MnCO_3$ from the literature [7, 11] we can estimate the absolute values of T_3: $T_1(T = 1.4\text{ K}) = 1100\ \mu s \rightarrow T_3(T = 1.4\text{ K}, T_n > 5\text{ K}) \simeq 8 \ldots 15\ \mu s$; $T_1(T = 4.2\text{ K}) = 750\ \mu s \rightarrow T_3(T = 4.2\text{ K}, T_n > 5\text{ K}) \simeq 20 \ldots 50\ \mu s$. Since these values are of same order of magnitude as the relaxation times obtained by spectroscopic methods, e.g. spin echo experiments [12] or parametric excitation of magnons [8, 9], we conclude that thermalization within the nuclear branch does not result from a diffusive many-step process but arises from only a few direct jumps from $k = 0$ to the range of large k and small $\mu_{n,k}$.

(iv) There occurs only a very weak dependence of T_3/T_1 on nuclear spin temperature, i.e. for an order of magnitude variation of T_n less than 50% change of T_3/T_1 (cf figure 7). This result can be taken as an indication that the thermalization of the nuclear branch does not arise from nuclear multi-magnon processes but is related to quasi-particles which are rather independent of the thermal occupation of the nuclear branch, i.e. to electron magnons or phonons. The influence of electron magnons on T_3 is supported by the experimental detail that different signs of ΔM can be observed in double resonance experiments, as mentioned above. Simultaneous excitation of AFMR, in principle, results in an extra contribution to ΔM arising from the electronic branch, but if the interaction of the uniform mode ($\omega_{e,k=0}$) with non-thermal nuclear magnons ($\omega_{n,k=0}$) is large, it will decrease T_3 and, as a consequence, also the main contribution to ΔM arising from the nuclear branch (see (9)). The competition of both effects can explain the different signs of ΔM.

5. Conclusion

The change of magnetic moment ΔM in the presence of RF pumping was investigated in the easy-plane antiferromagnet $MnCO_3$ by means of a SQUID device. The detailed analysis of different contributions has shown that the observed dependence of ΔM on external field, temperature, pumping power and frequency is only connected with the change of magnetic moment due to non-thermal nuclear magnons.

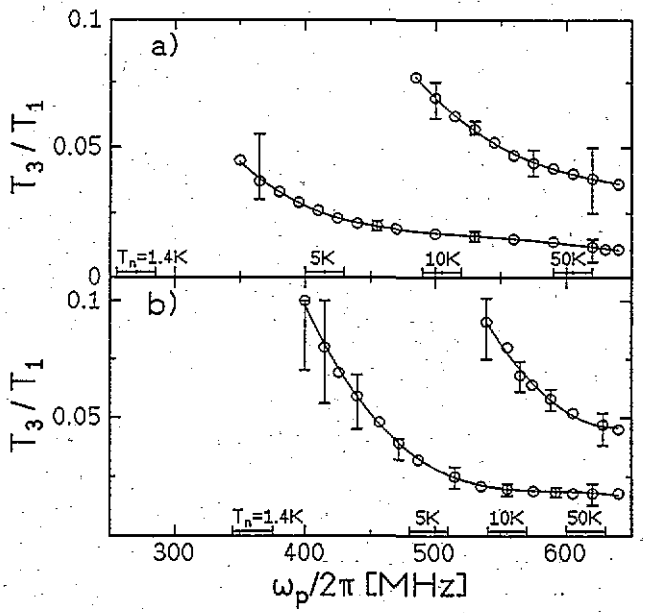

Figure 7. Experimental evaluation of T_3/T_1 corresponding to the decay of non-thermal nuclear k=0 magnons, (9), at $T = 1.4$ K and 4.2 K. (a) $H = 200$ Oe; (b) $H = 400$ Oe. Note that the data at 4.2 K and 1.4 K differ—like the temperatures—by a factor of about three.

The characteristic time T_3 describing the relaxation of these magnons into the whole nuclear dispersion branch could be evaluated from the experimental data. We found that T_3 is generally less than 10% of T_1 which is consistent with the assumption of a separate nuclear spin temperature T_n. The temperature dependence of ΔM shows that the ratio T_3/T_1 is proportional to T.

The quantitative evaluation of T_3 shows that thermalization within the nuclear magnon branch shows non-diffusive character. The weak dependence of T_3 on the nuclear spin temperature T_n implies that thermalization does not arise from nuclear multi-magnon processes. A possible explanation is related to a four-particle process where a non-thermal nuclear magnon ($k = 0$) interacts with an electron magnon or phonon resulting in a nearly degenerate electron magnon or phonon (because of the small energy range of nuclear excitations) and a nuclear magnon of large k (because of their large density of states). The efficiency of this process depends predominantly on the thermal occupation of the electron or phonon branch and only very weakly on the nuclear temperature. Since this process does not change the total number of nuclear excitations it does not influence the relaxation rate $1/T_1$, leaving T_3/T_1 rather small.

We hope that the present work will stimulate further theoretical investigations to obtain a better understanding of the detailed mechanisms of thermalization of magnons inside the nuclear branch.

Acknowledgments

We are grateful to A Maiazza for performing the EDAX analysis of our crystals. Stimulating discussions with A V Andrienko, M P Petrov, L A Prozorova and V L Safonov are gratefully

acknowledged. This work was supported by Sonderforschungsbereich 185 'Nichtlineare Dynamik' Frankfurt/Darmstadt and by the Alexander-von-Humboldt Stiftung.

References

[1] De Gennes P G, Pincus P A, Hartmann-Boutron F and Winter J M 1963 *Phys. Rev.* **129** 1105–15
[2] Suhl H 1958 *Phys. Rev.* **109** 606; Nakamura T 1958 *Prog. Theor. Phys.***20** 542–52
[3] Borovik-Romanov A S, Kreĭnes N M and Prozorova L A 1963 *Zh. Eksp. Teor. Fiz.* 45 64–70 (Engl. Transl. 1964 *Sov. Phys.–JETP* **18** 46–50)
[4] Borovik-Romanov A S and Tulin V A 1965 *Pis. Zh. Eksp. Teor. Fiz.* **1** 18–20 (Engl. Transl. 1965 *Sov. Phys.–JETP Lett.* **1** 134–6)
[5] Turov E A and Petrov M P 1972 *Nuclear Magnetic Resonance in Ferro- and Antiferromagnets* (New York: Wiley)
[6] Kotyuzhanskii B Ya and Prozorova L A 1990 *Sov. Sci. Rev.* A **13** 1–131
[7] Tulin V A 1968 *Zh. Eksp. Teor. Fiz.* 55 831–46 (Engl. Transl. 1969 *Sov. Phys.–JETP* **28** 431–8)
[8] Yakubovskiĭ A Yu 1974 *Zh. Eksp. Teor. Fiz.* **67** 1539–43 (Engl. Transl. 1975 *Sov. Phys.–JETP* **40** 766–8)
[9] Govorkov S A and Tulin V A 1977 *Zh. Eksp. Teor. Fiz.* **73** 1053–60 (Engl. Transl. 1977 *Sov. Phys.–JETP* 46 558–61)
[10] Lutovinov V S and Safonov V L 1979 *Fiz. Tverd. Tela* **21** 2772–83 (Engl. Transl. 1979 *Sov. Phys.–Solid State* **21** 1594–600)
[11] Lounasmaa O V 1974 *Experimental Principles and Methods Below 1 K* (London: Academic) ch 7
[12] Bun'kov Yu M and Dumesh B S 1975 *Zh. Eksp. Teor. Fiz.* **68** 1161–75 (Engl. Transl. 1975 *Sov. Phys.–JETP* **41** 576–82)